Advanced High Frequency AC Propulsion System for Next Generation Electric Hybrid Vehicle

論 文
2~1~2

Min-huei Kim

요 약

본 논문은 PNGV 계획에 따른 차세대 전기자동차의 개발을 위하여 고주파 교류 전력분배 시스템을 적용하여 이용 할 수 있는 추진력 장치의 구현 가능성에 대한 조사 연구이다. 실행 가능한 관점에서 전력분배와 에너지원의 결합이 쉽게 이루어 질 수 있고 변환이 가능한 여러 가지 형태의 시스템이 비교 검토 되었으며, 현재 기술 수준으로 보아 가까운 장래에 실현 가능한 최적의 시스템 구성은 배터리와 내연기관엔진 및 유도전동기를 이용하는 하이브리드형이 제시 되었다. 각 시스템의 원활한 전력수급과 운전특성를 위하여 단상 고주파 교류 전력분배 제어기법을 적용하였으며, 이 시스템의 타당성를 입증하기 위하여 시스템 구성에 따른 모델링과 컴퓨터 시뮬레이션을 실시하였다. 이 결과 차세대 전기자동차용으로 제시된 고주파 교류 전력분배에 의한 하이브리드형 추진력 시스템이 가능하며 운전특성도 우수함을 보여주었다.

Abstract - This paper describes a demonstration the viability of high frequency for ac propulsion power distribution system for next generation advanced electric/hybrid vehicle that tends to satisfy the PNGV (Partnership for Next Generation Vehicles) plans. In justifying this viability, different types of candidate distribution systems with the possible combinations of power and energy sources have been discussed and compared. The most viable system consisted of battery, internal combustion engine and induction machine has been suggested. A preliminary control strategy has been developed for the candidate single-phase high frequency ac system that modeling and computer simulation study have been made to validate the feasibility of the system performance. The study in the paper demonstrates the superiority of high frequency ac propulsion power distribution system for hybrid electric vehicle at least in the near future.

Key words : Electric hybrid vehicle, Induction motor, Vector control, HFAC power distribution system

I. INTRODUCTION

Electric vehicles (EV) were introduced practically from the beginning of this century. However, their importance for transportation was greatly diminished as gasoline-powered internal combustion engine continued to be improved and self-starter was commercially introduced. Petroleum fuel conservation and concern for environmental pollution are principal factors which are recently driving the worldwide research and development efforts for electric vehicles. In September 1993, the US Government along with the big three automakers (GM, Ford and Chrysler) declared a historic partnership program for next generation vehicles (PNGV) [1]. The salient PNGV goals which are expected to be fully implemented until 2003 can be summarized as follows:

- A state-of-the-art vehicle that has three times the present fuel efficiency (80miles/gallon)
- Emission level : 0.125/ 1.7/ 0/2 (HC/ CO/ Nox) (gms/mile)
- Acceleration : 0-100kmh (0-60mph) in 12 secs.
- Range : 610 km (280 miles)
- Capacity : 6 passengers
- Curb weight : 900 kg
- Luggage : 90 kg
- Drive train : 190 kg
- Useful life : 160,000 km (100,000 miles)

Although not mentioned as such, it has to be an hybrid electric vehicle (HEV) obviously with regenerative braking energy capture capability, in order to meet the desired fuel efficiency, range and emission. To achieve the PNGV goals at an acceptable consumer price, innovative and challenging research development in a number of related technologies will be needed [2][3].

Fig.1 shows the general block diagram for advanced propulsion power distribution system for next generation hybrid vehicle that can possibly meet the PNGV goals. Basically, it is a series hybrid system where the energy storage source and the power source contribute electrical power to a common bus that drives an ac motor through a variable voltage variable frequency (VVVF) converter. Traditionally, dc power distribution system has been considered for electric vehicle. Recently, NASA has demonstrated the viability of high frequency (20 Khz) single-phase ac power distribution system for aerospace applications [4] [5][6]. It appears that high frequency ac (HFAC) distribution for HEV has some special advantages [7].

Different types of energy storage and power devices shown in Fig.1 have been discussed [8]. The battery has been the traditional energy storage device, but flywheel or ultra capacitor can also be the alternate storage device. The superconducting magnet energy storge(SMES) can possibly be a viable source in the future, but it is very expensive at present. The battery or ultra capacitor can be directly connected to dc distribution bus, but needs an inverter for HFAC distribution system. On the other hand, a flywheel needs a dc machine (or converter-fed ac machine) drive for dc bus, or an ac machine with a frequency changer for HFAC bus. Normally, a gasoline engine is the power source for HEV, but other possible candidates may be diesel engine, gas turbine, Stirling engine or fuel cell. An engine/turbine can be connected to dc bus machine or to HFAC bus through an ac machine -frequency changer system. The ac machine can be induction, permanent magnet synchronous or switched reluctance type. However, in this study, the traditionally popular battery-gasoline engine-induction machine using single-phase HFAC bus will be considered. The main directions of power flow are given in the Fig.1. The various operation modes of the system can be summarized as follows:

- Mode 1 : Drive acceleration from the energy storage device
- Mode 2 : Drive deceleration by regenerative braking
- Mode 3 : Engine / turbine start-up from the storage device
- Mode 4 : Drive acceleration from power device
- Mode 5 : Drive acceleration by the combined power and energy storage device
- Mode 6 : Power source charging the storage device

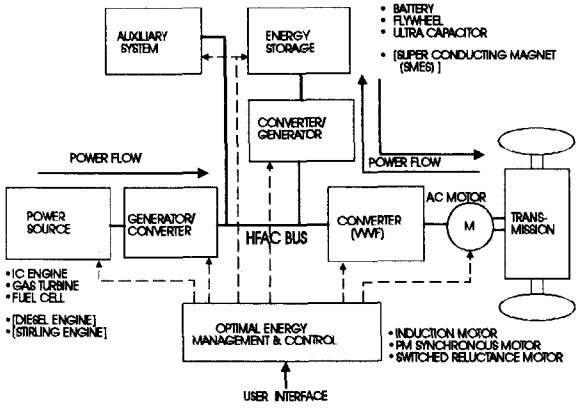

Fig. 1. Advanced propulsion power distribution system for next generation HEV

All the above modes of operation indicate that the control and energy management of the HEV system are very complex. A well-designed control methodology is to be formulated, based on analytical simulation study and implemented digitally with powerful DSP's.

II. CANDIDATE ENERGY STORAGE AND POWER SOURCE SYSTEMS

1. Battery

Electric storage battery has been the "heart and soul" of EV even from the beginning of this century when EV was first introduced. Among all the components of the EV propulsion system, the power electronic and machine control technology have been well developed, but the battery still remains the weakest link in the system. For this reason, battery has been the prime focus of research and development for long time. In 1990, the US Advanced Battery Consortium(USABC) was established to systematically sponsor research and development activities for EV battery technology. Table 1(Appendix) gives the battery technology status in the USABC established [8].

The lead-acid battery is possibly the best compromise in energy density, power density, life-cycle, cost and other criteria. It has been

widely used in the past and present projects, and will possibly remain so in the near future. Lead-acid batteries are easily available in mass scale, but are not yet in high volume production. It can be shown that 40-50 miles range in urban driving is easily possible with lead-acid battery that will be exceed 30% of vehicle curb weight.

Nickel-Cadmium battery is more expensive because of raw material costs. But it has relatively high energy density, power density and long life compared to lead-acid battery. Many Japanese EV projects prefer Ni-Cd battery. Cadmium is not environmentally safe and recycling may be a problem.

2. IC Engine

For long time, the spark-ignition internal combustion engine (IC engine) has been known as the traditional power source for the general gasoline-powered vehicle. Modern turbo-charged engine improved by microprocessor-controlled fuel injection has small size and high efficiency. It is possibly the best candidate for HEV power source, and will remain so in the early of the next century.

3. IC Engine - Battery system

This is the traditional distribution system in a hybrid vehicle, and it will possibly remain most viable in the near term (up to the early part of the next century). Spark-ignited homogeneous charge reciprocating type IC engine has long been the standard power source for a passenger automobile. The engine has gone through allow evolutionary improvement over a long time. In a series hybrid system, the engine can operate independently at optimal speed for the best possible efficiency. The diesel engine, although has high efficiency, is not favored because of exhaust odor and fumes, higher noise level and higher first cost of diesel car. The Stirling engine has the advantages of silent operation, low exhaust emission level, superior fuel economy at steady state operation, and ability to operate on any liquid fuel. However, the disadvantages are that it is very expensive, have large warm-up time, and poor performance in urban driving cycle.

Although today's propulsion battery is considered too bulky, too expensive and has low life cycle. The battery types which are under considerably for EV/HEV are : Lead-Acid, Nikel-Cadmium, Sodium-Sulfur, Zinc-Air, Lithium-polymer, Nickel Hydride, Nickel Iron, Zinc Bromide, Sodium Nickel Chloride, Nickel-Zinc, Nickel Hydrogen and Lithium Iron Disulfide. Presently, lead-acid battery is possibly the best compromise in specific energy (wh/kg), specific power (w/kg), life cycle, cost ($/kwh) and other criteria although Ni-Cd and Na-S batteries have been widely used.

Based on the characteristics of the individual energy storage and power devices, the corresponding interface machine-converter needed to connect the distribution bus, a general comparison table for the candidate systems is given in Table 2(Appendix). Note that the numerical comparison is difficult where the right technology is not there or the product is not yet available in the market. It is given for general guidance to the reader. From overall comparison in the table, it appears that gasoline engine-battery system is the most viable candidate in the near-term (next 10 years) technology perspective.

III. HIGH FREQUENCY AC DISTRIBUTION

The power supply distribution system in hybrid vehicle interconnecting the energy storage device, power device and the propulsion motor can be based on dc, resonant link dc or high frequency ac system that can be based on single-phase or polyphase. Whatever the case may be, the system should be optimally designed for cost and performance considering the characteristics of the system components. Fortunately, in hybrid vehicle, all the components are in close proximity. Consequently, modular design with minimum wiring length is easily possible, single-phase high frequency ac system for HEV has the singular advantage [2][6].

1. Single-Phase HFAC

The high frequency single-phase ac link distribution system under consideration in the present study is shown in Fig.2. The system uses battery as the energy storage device and gasoline engine as the power device. Both the motor and the generator use the cage type induction machine and the converters use IGBT switches.

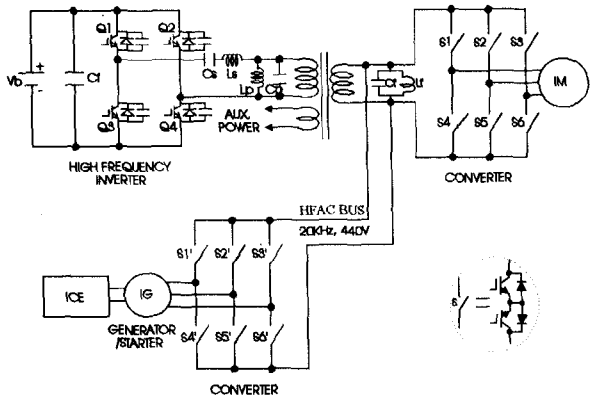

Fig. 2. Single-phase HFAC distribution system

Tentatively, 20 KHz, 440 V HFAC distribution system (as considered for space application) will be assumed. The battery voltage is inverted to HFAC through a H-bridge resonant inverter. The magnitude of the sinusoidal resonant voltage is controlled by phase angle modulation of inverter legs that generate quasi-square wave at the inverter output. The inverter outout voltage is boosted with isolation by high frequency transformer, and then supplied to the converters which feed the drive motor and generator, respectively, at variable voltage and variable frequency. The converter switches have to withstand ac voltage and conduct current in both directions. The equivalent ac switch configuration using inverse- series IGBT's with bypass diodes is indicated in the figure. The integral ac switch is not yet available commercially, but device manufactures confirm that such switches with "smart" capability can be made available at economical price if sufficient demand exists. The converters switch at zero voltage, and corresponding advantages of soft-switching can be summarized as follows:

- The switching loss is practically eliminated.
- This improves converter efficiency.
- Less converter loss demands less cooling.
- Less loss permits easy integration of the inverter.
- The devices practically do not need any snubbing. Consequently, component count is reduced and reliability is improved.
- The device switching stress is low in normal and fault conditions improving its mean time before failures (MTBF).
- The acoustic noise in the magnetic is eliminated.
- The EMI problem is less because of soft rise and fall of PWM voltage pulses.
- Low dv/dt is beneficial for the devices and machines.

2. Distribution frequency and voltages

If single-phase HFAC system is assumed to be viable at this point, the question arises what frequency and voltage is optimum for the system. For aerospace application, 20 KHz, 440 V system has been considered. As the IGBT switching speed is improving and voltage rating is increasing, there will be a tendency to increase the level of frequency and the voltage. In general, higher frequency has the following advantages:

- The high frequency power transformer and other passive circuit components become smaller. Instead of using ferrite, future potential use of amorphous metal has the further advantage of higher flux density, and correspondingly, smaller size. However, this size reduction can not be extended too far for magnetic material, because higher loss density will demand adequate surface area for cooling.
- Harmonic ripple current in the machines will decrease improving the efficiency. This improvement will be slightly offset by the increase of harmonic core loss.
- The harmonic filter size for the battery will decrease.
- Auxiliary power supply units will be smaller and their efficiency will be improved.

However the disadvantages are:

- The power device needs higher switching speed. Otherwise, device switching will tend to occupy larger angular interval and make soft switching difficult.
- The dv/dt withstand capability of the devices and the machines should be high.
- Higher dv/dt increases displacement current in machine insulation, and thus, deteriorate its life.
- The EMI effect will be worsen.

Selection of higher link voltage (independent of battery voltage) will permit higher voltage rating of the machines for the same power rating. This

decreases the machine copper volume but increases the iron volume. The machine will be very economical with improvement of efficiency. The increase of voltage rating and the corresponding decrease of current loading will also economize the converter cost and improve its efficiency. However, increase of machine harmonics will tend to increase the harmonic loss offsetting the efficiency advantages. The use of MCT has distinct advantage because of lower conduction drop. As IGBT switching speed is further improved in future, or other high frequency devices can be boosted conveniently. These will make the system more economical and give better performance.

IV. CONTROL SYSTEM

1. Design for component size

In order to make the valid of the HFAC distribution systems, approximate sizing calculation of the components was made for under similar assumptions[2][9]. The assumptions were based on current or near-term technology. The details of calculation are beyond the scope of this paper. The drive induction motor is rated at 100kw (peak power), 4-pole, base speed of 6,435 rpm and the maximum speed of 15,000 rpm. However, the machine fundamental voltage ratings are different, and are dictated by the respective input voltage. The battery is assumed to share rightly 70% of the power(70Kw) and the engine shares the rest (30 Kw), as indicated in Fig.3.

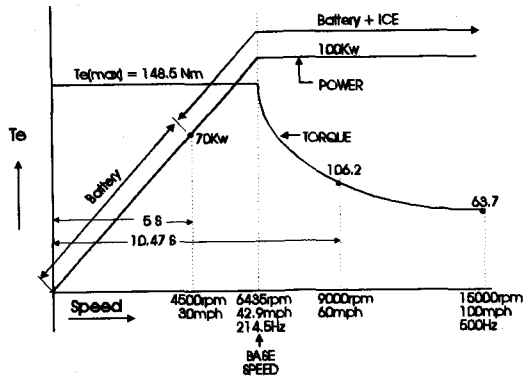

Fig. 3. Driver motor operation characteristics

Lead-acid type battery of nominal 300V rating was selected, and the battery voltage is assumed to vary between 210V and 390V. Note that in HFAC system, the battery will be more economical because of lower voltage rating. The battery storage capacity of 8 KWh was selected so that the HEV can be used as zero emission EV in city driving for the range of 55 miles and acceleration capability of 0-30 mph in 5 secs. The battery in conduction with the engine permits acceleration of 0-60 mph in 10.47 secs (PNGV goal is 12 secs). The capacitor filter (C_f) was selected to be ac type for high reliability and long life. The induction generators located in both side of the system are assumed to operate at constant speed of 5000 rpm (base speed), and variable power is generated at variable torque. The generator fundamental voltage rating is dictated by the respective converter input voltage. Both machines were operated in vector control mode [10].

The silent points in the component sizing can be discussed as follows:

- The link voltage was boosted and regulated to be constant. On the basis of 440V link voltage, the machines fundamental voltage rating is 235V. High voltage rating with the correspondingly reduced current rating makes the machine more economical and efficient.
- The driving converter also consists of 12 IGBT's, and each one is rated at 1000 V, 400A on the basis of 440 V link voltage. The extra voltage margin on the devices allows the link voltage to be boosted to 600 V. This permits selection of one size lower IGBT (i.e., 1000 V, 300 A) and the machine voltage can be boosted to 324 V.
- The corresponding voltage rating should be designed on the basis of 622V peak line voltage.
- The filter capacitor (C_f), based on 10% second harmonic (40 KHz) injection in the battery, is calculated to be 1.74 uF.

2. Control of Converter-Motor

The drive motor is controlled by indirect vector control method, as shown in Fig.4. In the outer loop, it is a torque-controlled system where the torque component of current I_{qs}* (proportional to torque) is controlled by the potentiometer. The rotor flux is constant in the constant torque

region, and it is controlled by the flux component of current I_{ds}*, as shown. The slip frequency signal W_{sl} is proportional to I_{qs}* by the slip gain factor Ks. The speed signal W_r is added to the slip signal W_{sl} to generate the frequency command W_e which is then integrated to generate the unit vector signals through the function generators.

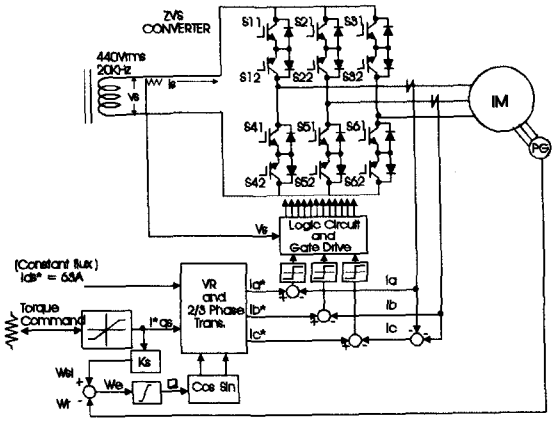

Fig. 4. Control block diagram of motor drive system

Both the signals I_{qs}* and I_{ds}* are then vector-rotated and converted to three-phase current command, as shown.

The phase currents are controlled independently by discrete half-cycle pulse width modulation (also known as Delta modulation), as shown in Fig.5.

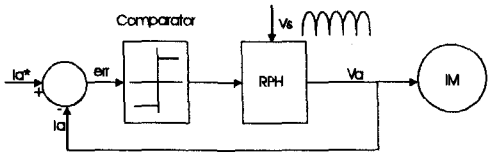

Fig. 5. Block diagram for current regulated delta modulation

As the polarity of phase current error (err) changes and exceeds a threshold value, the converter is ready to change the switching pattern. However, since the convertter is constrained to have zero voltage switching (ZVS), it waits until the next zero crossing interval is identified. The resonance pulse hold (RPH) produces half-cycles of resonant pulses which have periodic zero crossing. The equivalent half-bridge converter with respect to the hypothetical center- point of HFAC voltage v_s. already discussed[6]. Fig.6 explains the control principle in detail. The HFAC voltage wave v_s is processed and logic pulse train(L) is generated which gives the permissible window time for switching of the devices. The logic signal K corresponds to the polarity of err signal and NA is the logical interval for switching. Note that NA wave is delayed because of the time delay for zero voltage switching. The phase voltage v_{an} (with respect to the center-point) appears like a "square wave", but it is further dictated by the polarity of v_s signal.

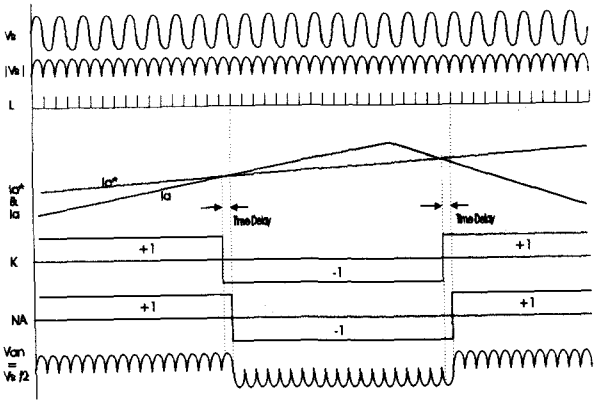

Fig. 6. Operation of one phase converter

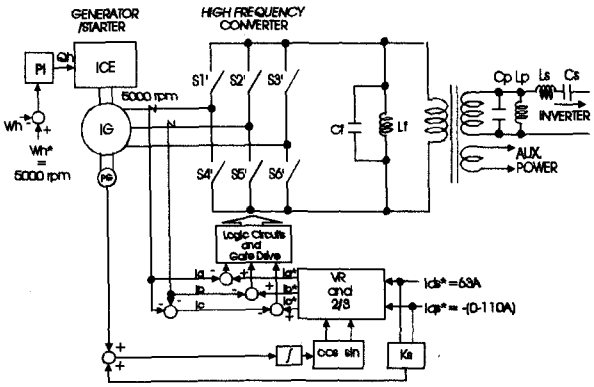

Fig. 7. Control block diagram of ICE and generator

3. Control of Converter-Generator

The control principle of converter-generator is essentially similar to the converter-motor system, and is shown in Fig.7. The same induction machine, as shown in Table 3, is considered for control development and simulation study. The ICE is initially started with the generator operating in motoring mode. As the ICE starts, its

Table 3: Parameters for 100 Kw (peak power) machine

Line Voltage = 240 V
Poles = 4
Rated i_{ds} = 63 A
Rated i_{qs} = 278 A (50Kw)
Peak i_{qs} = 556 A
Rated Stator Current = 202 A
Maximum Speed = 15,000 rpm
Power Factor = 0.8
Stator Resistance (R_s) = 0.01121 Ohm
Rotor Resistance (R_r) = 0.01243 Ohm
Stator Leakage Inductance (L_{ls}) = 0.001314 mH
Rotor Leakage Inductance (L_{lr}) = 0.001314 mH
Magnetizing Inductance (L_m) = 2.13 mH

speed is raised and locked to the constant speed of 5000 rpm. The programmable speed control for optimization of ICE efficiency is also possible. The speed loop operates independently with the control of throttle angle, as indicated in the figure. Once in generating mode at constant speed, the variable power of the generator is controlled by variable torque by manipulation of Iqs (negative). In actual system, feedforward power injection will be needed to minimize fluctuation of HFAC voltage.

4. Control of Resonant Inverter

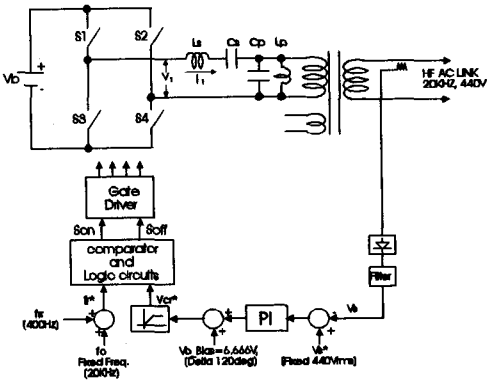

Fig. 8. Control block diagram of resonant inverter

Fig.8 shows the control block diagram of the resonant inverter. The two legs of the H-bridge are controlled at variable phase angle to generate the quasi-square wave so as to regulate the output fundamental voltage irrespective of the battery voltage and load variation. The inverter operates with close loop voltage control with the feedback voltage signal derived from the HFAC link through a rectifier and lowpass filter. The error voltage through a PI (proportional - integral) controller is added to the bias voltage signal to constitute the V_{cr}* signal , as shown. Since the inverter is to operate at slightly lagging power factor, the ideal HFAC frequency (20 KHz) is added with f_{rr} (400 Hz) to generate the actual frequency command (f_r). A control sawtooth wave is generated at frequency f_r, as shown. The bias voltage signal is generated such that the inverter operates at delta angle of 120 deg. at 300V battery voltage. The angle will increase at lower voltage whereas it will decrease at higher voltage. The generation of IGBT gate drive signals for generation of quasi-square wave is indicated in the figure. The control circuit was valid for motoring mode of the drive system.

5. Developed Control System

The developed control of the total system is shown in Fig.9.

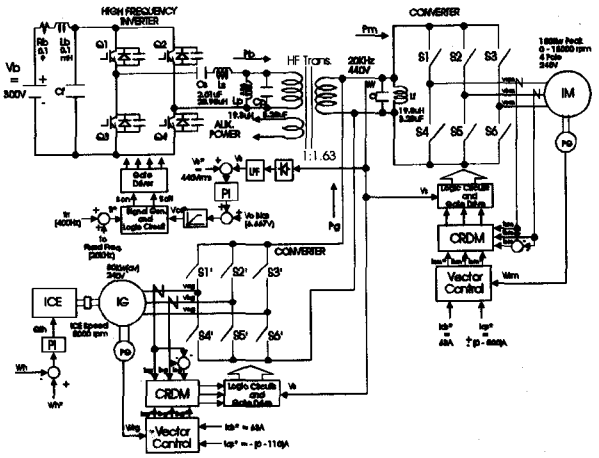

Fig. 9. Control block diagram of the total system

V. MODELING AND SIMULATION

A preliminary modeling and simulation study of the candidate HFAC system given in Fig.2 has been described in this section. The study is based on the numerical component sizing and control development described before. The performance of the system could be improved significantly by

improvement of the control strategy but it could not be possible within the time constraint of the project. The language SIMNON (Engineering Software Concepts) was used for simulation. Initially, the total system was subdivided into several sub-systems, and modeling and simulation study was made on each sub-system[11]. Finally, when each sub-system was operating successfully, the total system simulation was studied.

1. Battery - Resonant Inverter (Sub-System 1)

The sub-system 1, as shown in Fig.8 and 9, was first taken into consideration. The HFAC link supply (440V, 20 KHz) only was generated by the open-loop voltage control of the resonant inverter for this simulation study[12][13][14], and was terminated by passive RL load (Z=0.6+J0.8 Ohms). Only nominal battery voltage(300V) that generates a quasi-square wave voltage at delta angle of 120 degree was considered. Fig.10 shows the V_{do} (carrier vave), V_{cr}*, v_l, i_l, v_s and i_s waves at ideal 20 KHz frequency with δ=120 degree (i.e. V_{cr}= 6.667V). The currents i_l and i_s lag with respect to their fundamental components of voltage. Both the current waves i_l and i_s are in phase except the amplitude difference because of the transformer.

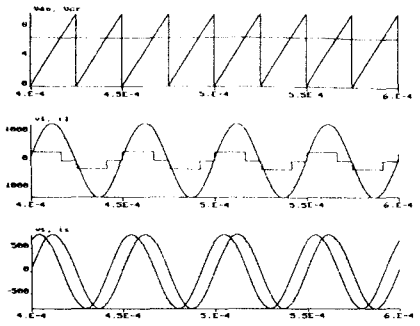

Fig. 10. Waveforms of resonant inverter

2. HFAC-Converter-Induction Motor (Sub-System 2)

The configuration for this sub-system is shown in Fig.4. An ideal HFAC source was considered for this study. The induction motor was represented by dynamic d-q model (synchronously rotating reference frame). A Delco Remy 100KW (peak power) machine designed for EV drive was taken for the simulation study. The machine parameters are shown in Table 3.

As mentioned before, the EV drive is essentially a torque-controlled system. But, for the convenience of simulation study, a speed controlled system was adapted by modified the figure that add a speed feedback control system using PI controller. Fig.11 shows the simulation results of speed control for sub-system 2 ; (a) the speed loop response, v_s and i_s waves, (b) the corresponding current and torque responses. The torque component of current i_{qs} remains saturated (500A) during acceleration, and then falls to the steady state value as demanded by the steady state load torque (T_L), but the magnetizing current ids always remains constant at 63A. (c) the machine phase voltages that the corresponding waveforms at expanded scale. (d) the expanded view of HFAC voltage, current and instantaneous power waves. The current is flat-topped and highly distorted which has low distortion factor but near unity displacement factor. It also contains small amount of sub-harmonics. The instantaneous power wave is fluctuating, as expected.

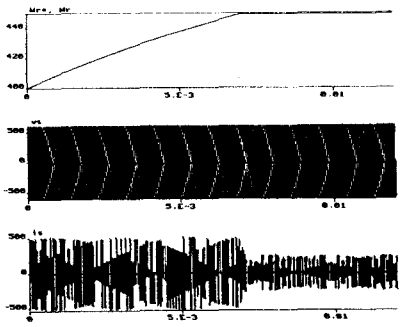

(a) Speed loop response (top), HFAC bus voltage v_s (middle) and current i_s (bottom)

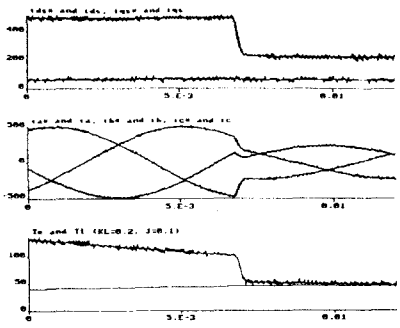

(b) i_{ds}* & i_{ds} and i_{qs}* & i_{qs}(top), three-phase current(middle) and torque T_e & T_L(bottom)

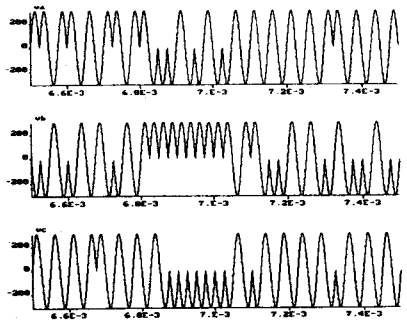

(c) Expanded waveforms of three-phase voltage v_a, v_b and v_c

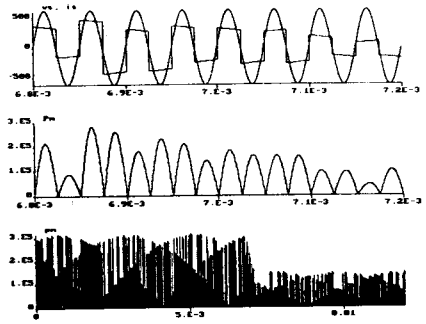

(d) Expanded view of HFAC voltage, current and instantaneous power wave

Fig. 11. Simulation results of the speed control for sub-system 2

Fig.12 demonstrates motoring and regeneration mode of operation of the drive. The corresponding waveforms are shown in detail in the figures. The phase of current is changes from motoring to regeneration, and the corresponding average power becomes negative.

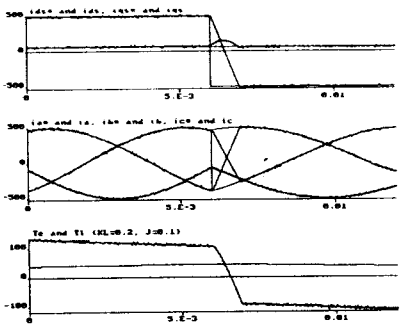

(a) i_{ds}* & i_{ds} and i_{qs}* & i_{qs}(top), three-phase current(middle) and torque T_e & T_L(bottom)

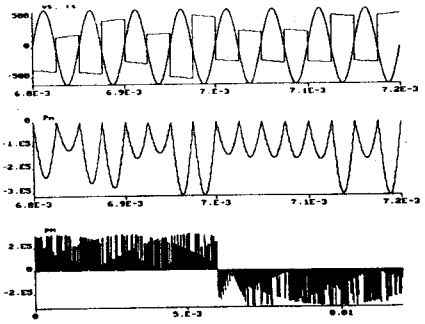

(b) Expanded view of HFAC voltage, current and instantaneous power wave

Fig. 12. Operation of motoring and regeneration mode for sub-system 2

3. Battery-Inverter-Converter-Induction Motor (Sub-System 3)

The sub-systems 1 and 2 are cascaded to constitute the sub-system 3. It is definitely a more complex system demanding sophisticated control. Note that the resonant inverter has been controlled with close loop voltage control and a resonant filter has been added at the input of the motor converter to trap the current harmonics, as shown the Fig.9. The system has been studied only for steady state condition.

Fig.13 shows the simulation results of speed control for sub-system 3 ; (a) the speed(W_r* & W_r), voltage vcr and the inverter voltage loop response. The machine shaft has high inertia, and therefore, the speed change from initial speed is minimal within 10 ms time interval. (b)-(e) show the corresponding currents, phase voltages, HFAC link voltages and currents, torque and power waves. The corresponding expanded waves are shown in (f)-(g). In the absence of any control sophistication, the HFAC voltage wave is distorted and varies widely, but it does not affect the motor performance and does not exceed the safe limit. A feedforward instantaneous power control will alleviate this condition. Again, near-unity displacement factor condition has been demonstrated by the vs and is waves.

4. Total System

The total system under simulation study is shown in Fig.9. It consists of sub-system 3 added with the ICE-generator-converter subsystem

(sub-system 4). The sub-system 4 is essentially the same as that of sub-system 2, and therefore, it will not be discussed separately. The total system was studied at steady state condition for the ICE speed of 5,000rpm and the motor speed of 2000rpm (about) with both under feedback control. Fig.14 shows simulation results of the suggested total system; (a) the speed of ICE(generator) and motor, V_{cr}* wave and HFAC bus the inverter voltage loop performance. (b) and (c) show the motor currents and the phase voltage waves, respectively. The corresponding waves for the generator are shown in (d) and (e). (f) shows the motor and generator torques indicating that the motor torque is positive but the generator torque is negative. (g) and (h) show the distribution of HFAC link currents between the motor and the generator, and expanded waveforms. (i) shows the corresponding distribution of HFAC link powers. The satisfactory operation of the system is obvious in spite of the modulation of HFAC voltage, current and power waves.

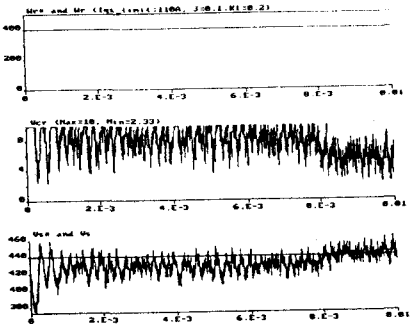

(a) Speed (W_r* & W_r, top), voltage V_{cr} (middle) and HFAC bus voltage v_s(bottom) of inverter loop response

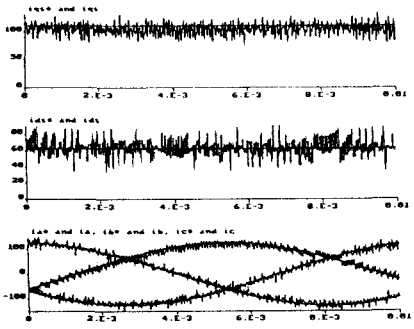

(b) i_{qs}* & i_{qs} (top), i_{ds}* & i_{ds}(middle) and three phase current i_a, i_b & i_c (bottom)

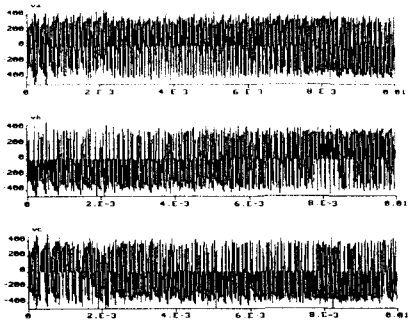

(c) Three phase voltage waveforms v_a, v_b and v_c

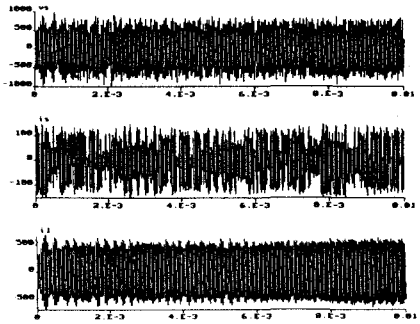

(d) HFAC voltage v_s (top), current i_s (middle) and resonant current i_l waveform(bottom)

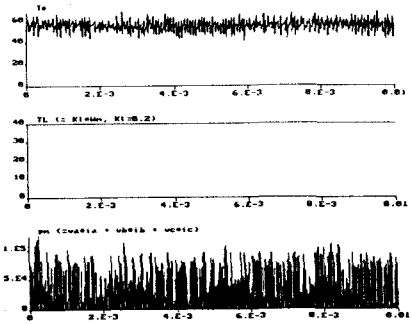

(e) Torque T_e(top), T_L(middle) and instantaneous power(bottom)

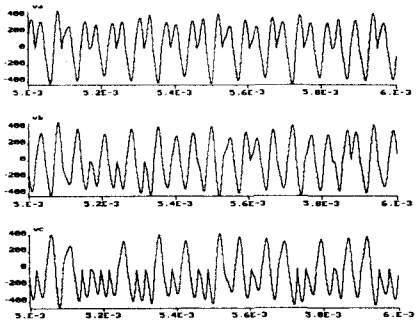

(f) Expanded waveforms of (c)

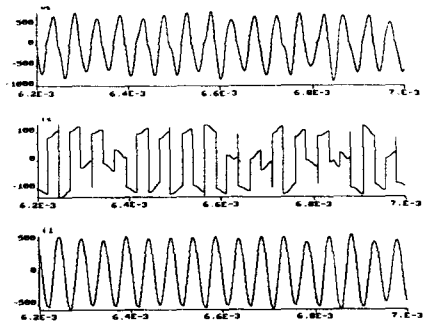

(g) Expanded waveforms of (d)

Fig. 13. simulation results of speed control for sub-system 3

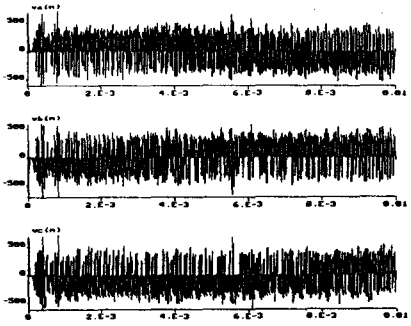

(c) Three phase voltage waveforms v_a, v_b and v_c of induction motor

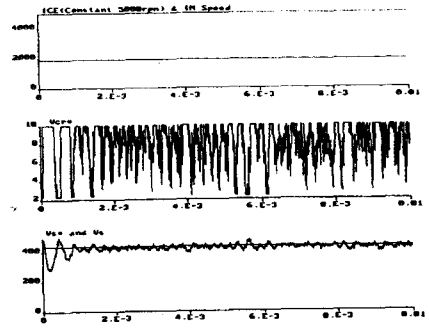

(a) Speed of ICE(generator) & motor(top), voltage V_{cr}(middle) and HFAC bus voltage v_s(bottom) of inverter loop performance

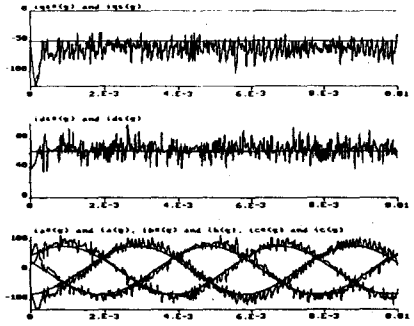

(d) i_{qs}* & i_{qs} (top), i_{ds}* & i_{ds} (middle) and three phase current i_a, i_b & i_c (bottom) of induction generator

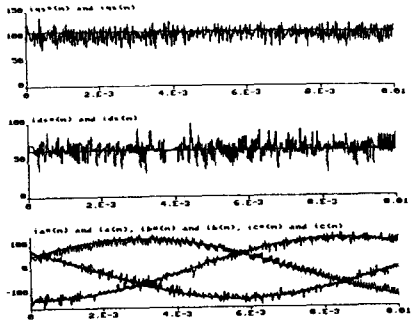

(b) i_{qs}* & i_{qs} (top), i_{ds}* & i_{ds} (middle) and three phase current i_a, i_b & i_c (bottom) of induction motor

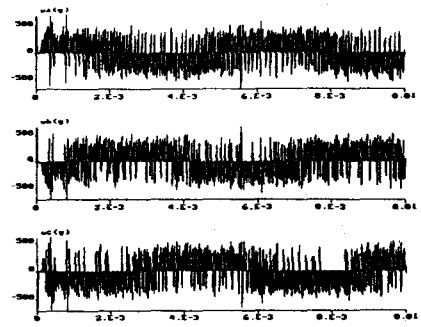

(e) Three phase voltage waveforms v_a, v_b and v_c of induction generator

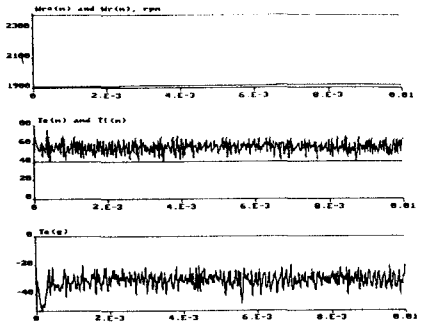

(f) Speed W_r* & W_r of motor(top), Torque T_e & T_L of motor (middle) and T_e of generator

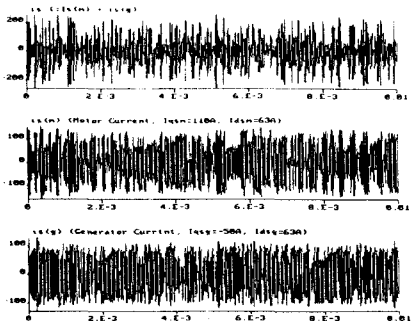

(g) Waveforms of HFAC bus current, total current i_s ($=i_{sm}+i_{sg}$, top), motor current (i_{sm}, middle) and genertor current (i_{sg}, bottom)

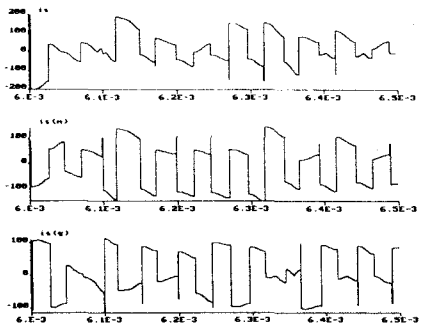

(h) Expanded waveforms of (g)

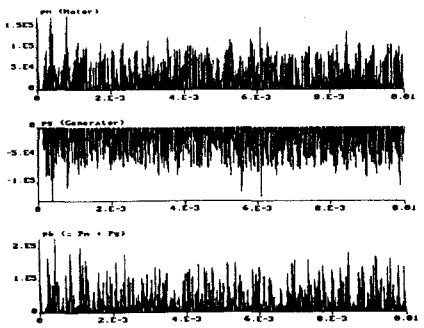

(i) Instantaneous power waveforms, motor power p_m(top), generator power p_g(middle), total power p_b ($=p_m+p_g$, bottom)

Fig. 14. Simulation results of the suggested total system

VI. CONCLUSION

This paper presents a demonstration the viability of the single-phase high frequency ac distribution system for next generation advanced hybrid electric vehicles that tends to satisfy the PNGV goals. The candidate system with battery, gasoline engine and HFAC distribution have been identified and developed for the resonant inverter, converter-motor, converter-generator and internal combustion engine as the most viable in near-turn technology. The components of the system have been modeled and studied by simulation. The simulation study has been made initially on the component sub-systems, and then finally on the total system. As usual, the injected converter current in HFAC link are flat-topped which are rich in harmonic content. In the system, power flow is fluctuating and the mismatch of generated power with consumed power tends to cause fluctuation of link voltage with added distortion. Feedforward power compensation is needed to alleviate this condition. However, in spite of distortion and modulation of HFAC voltage, the converter were functioning satisfactorily generating good quality current-controlled PWM waves. Although 20KHz, 400v system was considered for the study, it appears that there are additional advantages for selecting higher voltage and higher frequency. Higher link voltage with higher frequency, will make both converter and machine more economical, improve efficiency, and filter size becomes more demanding within a short window-time witch will be hopefully met by the next generation high speed devices. Finally, a preliminary control strategy of the high frequency ac propulsion system was designed and some simulation study was made to validate the system operation. The system was found to perform well in spite of some modulation of the ac link voltage.

This research was supported by the Yeungnam Junior College Research Grants in 1996.

REFERENCES

[1] US Government, "Partnership for Next Generation of Vehicles (PNGV) Program Plan", July 1994.

[2] Bimal K. Bose and Min-Huei Kim, "Advanced propulsion power distribution system for next generation electric/hybrid vehicle, Phase 1: Preliminary system studies", Final Report Submitted to NASA Lewies Research Center, June 1995.

[3] L. Chang, "Recent developments of electric vehicle and their propulsion systems", IEEE Trans. on AES System Mag., pp. 3-6, Dec. 1993.

[4] I.G. Hansen and G.R.Sundberg, "Space station 20khz power management and distribution system", IEEE-PESC Conf., pp. 676-683, 1986.

[5] P.K. Sood and T.A. Lipo, "Power conversion distribution system using a high frequency ac link system", IEEE Trans. on IA, Vol. 24, pp. 288-300, Mar./Apr. 1988.

[6] I.g. Hansen, "Description of a 20 khz power distribution system", 21st Intersocietyenergy Conv. Engg. Conf. Rec., pp. 1893-1895, Aug. 1986.

[7] Min-Huei Kim, B.K. Bose and M.D. Kankam, "High frequency ac vs. dc distribution system for next generation hybrid electric vehicle", IEEE-IECON'96, pp. 706-712, 1996

[8] X. Xu and V. A. Sankaran, "Power electronics in electric vehicles challenges and opportunities", IEEE-IAS Annu. Meet. Conf. Rec., pp. 463-468, 1993.

[9] R.A. weinstock et al., "Optimum sizing and selection of hybrid electric vehicle components", IEEE-IAS Annu. Meet. Conf. Rec., pp. 251-256, 1993.

[10] S. K. Sul and T.A. Lipo, "Field oriented control of an induction machine in a high frequency link power system", IEEE Trans. on Power Electronics, Vol. 5, pp. 436-445, Oct. 1990.

[11] J.S. Lai and B.K. Bose, "An induction motor drive using an improved high frequency resonant dc link inverter", IEEE Trans. on Power Electronics, Vol. 6, pp. 504-513, July 1991.

[12] S. kondo et al., "Resonant link dual converter system for motor drives", IEEE-IAS Annu. Meet. Conf. Rec., pp 789-784, 1991.

[13] P.Jain and M. Tanju, "A 20 khz hybrid resonant power source the space station", IEEE Trans. on AES, Vol. 25, pp. 491-496, July 1989.

[14] D.M. Divan and G. Skibinski, "Zero switching loss inverters for high power applications", IEEE-IAS Annu. Meet. Conf. Rec., pp . 627-634, 1987.

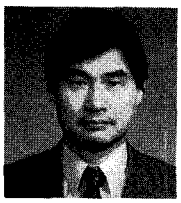

Min-Huei Kim (金玟會) was born in Kyung-Buk province on July 23, 1951. He received the B.S. and M.S. degree in electrical engineering from Yeung-Nam University in Teagu, and Ph.D. degree from the University of Chung-Ang in Seoul, in 1973, 1979 and 1988, respectively. In 1979, he joined an Instructor of the Yeung-Nam junior College in Teagu, and is currently a professor in Department of Electrical Engineering. From 1993 to 1995, he worked as a visiting professor in Power Electronics Application Center at The University of Tennessee, Knoxville. He received a award that "The IEEE Industrial Electronics Society proudly awards First Prize in the IECON'96 Best Paper Competition".

Dr. Kim's research interests are a control system of motor drives, power converters, neural networks and it's application of power electronics. He is a member of KIEE, KITE, KIPE, JIEE and IEEE.

APPENDIX

Table 1. Battery technology status

Technology		Cell Voltage Volts	Operating Temp. C	Specific Energy Wh/Kg 3H rating	Energy Density Wh/L	Specific Power W/Kg	Power Density W/L	Life Cycle [Years]	Cost $/Kwh	Energy Eff. %
NEAR Term Battery	Lead Acid	2.1	3.5 to 70	35	80-90	125-230	230-600	500(3)-600(4)	70-130	-
	Nickel Cadmium	1.25	-30 to 50	55	120	190	330	2000(10)	600	-
MID Term Battery	USABC Goals		-30 to 65	80-100	135	150-200	250	600(5)	<150	-
	Nickel Metal Hydride	1.4	-20 to 60	65	175	150	400	600(2)	-	80
	Sodium Sulfur	2.08	300-400	85	115	120	180	350(2)	600	91
	Sodium Nickel Chlorride	2.59	250-350	130	170	168	225	1000(5)	-	-
LONG Term Battery	USABC Goals		-40 to 85	200	300	400	600	1000(10)	<100	-
	Zinc Air	1.62	25-65	130	120	50	65	70	110	-
	Lithium Iron Disulfide	1.62	400-450	165	240	375	550	500(2)	110	-
	Lithium Polyer	2.8-4.5	0-100	160	260	200	210	300(1)	200	-
	Nickel Iron	-	-	50	118	100	-	900	200	58
	Nickel Zinc	-	-	67	142	105	-	114	-	77
	Zinc Bromine	-	-	79	56	40	-	334	-	75
	Lithium monosulfide	-	-	66	133	64	-	163	-	81

Table 2. General comparision of candidate distribution system

Item	ICE-Batt.	ICE-UC	GT-Bat.	GT-UC	ICE-FW	GT-FW	FC-Bat.	FC-UC	FC-FW
Cost(pu)	1	1.5	1.3	1.8	1.2	1.5	2	2.5	2.2
Weight(pu)	1	1.5	1.1	1.6	0.8	0.9	2	2.5	2.2
Emission	medium	medium	small	small	medium	small	small	small	small
Availability	good	not good	good	not good	good	good	not good	not good	not good
Practicality	good	not good	good	not good	good	good	not good	not good	not good
Efficiency(pu)	1	1.05	0.8	0.85	0.8	0.7	1.2	1.25	0.9
Safety	good	good	medium	medium	not good	not good	good	good	not good
Noise	medium	medium	medium	good	medium	medium	none	none	medium
Control Coplexity	medium	medium	high	high	high	high	small	sll	medium
EV Range(pu)	1	0.7	1	0.7	0.7	0.7	1	0.7	0.7
Total Range(pu)	1	1	1.1	1	1	1.1	1.1	1.1	1.1
Comments	Avilable technology	Needs R & D	Needs R & D	Needs R & D	Available technology	Needs R & D	Needs R & D	Needs R & D	Needs R & D

* Numerical figures in the table should not be taken seriously where right technology is not avilable.
* ICE : Internal Combustion, UC : Ultra capacitor, GT : Gas Turbine, FW : Flywheel, FC : Feul Cell, Batt. : Battery